



Calhoun: The NPS Institutional Archive
DSpace Repository

Faculty and Researchers

Faculty and Researchers Collection

2003

Hydrostatic Consistency in Sigma Coordinate Ocean Models

Chu, Peter C.; Fan, Chenwu

<http://hdl.handle.net/10945/43392>

Downloaded from NPS Archive: Calhoun



Calhoun is a project of the Dudley Knox Library at NPS, furthering the precepts and goals of open government and government transparency. All information contained herein has been approved for release by the NPS Public Affairs Officer.

Dudley Knox Library / Naval Postgraduate School
411 Dyer Road / 1 University Circle
Monterey, California USA 93943

<http://www.nps.edu/library>

Hydrostatic Consistency in Sigma Coordinate Ocean Models

Peter C. Chu and Chenwu Fan

Naval Ocean Analysis and Prediction Laboratory, Department of Oceanography

Naval Postgraduate School, Monterey, California

Abstract

Truncation error and hydrostatic inconsistency at steep topography are two concerns in sigma coordinate ocean models due to the horizontal pressure gradient being difference of two large terms. A consensus is reached in the ocean modeling community on the first concern (truncation error), but not on the second concern (hydrostatic inconsistency). Since the integration of the pressure gradient over a finite volume equals the integration of the pressure over the surface of that volume (always dynamically consistent), dynamical analysis on finite volumes is used to determine the hydrostatic consistency of a sigma coordinate ocean model. A discrete, hydrostatically consistent scheme is obtained for the sigma coordinate ocean models. Comparison between finite-volume and finite-difference approaches leads to the conclusion that a Boussinesq, hydrostatic, sigma coordinate ocean model with second-order staggered scheme is always hydrostatically consistent. Guidance for improving numerical accuracy is also provided.

1. Introduction

In regional oceanic (or atmospheric) prediction models the effects of bottom topography must be taken into account and a continuous topography is implied in terrain-following sigma coordinates. The water column is divided into the same number of grid cells independence of depth. We restrict attention to two dimensions. Let (x, z) denote Cartesian coordinates and (x^*, σ) be the sigma coordinates. The conventional relationship between z - and sigma-coordinates is given by

$$x = x^*, \quad z = \sigma H(x^*), \quad (1)$$

where z and σ increase vertically upward such that $z = \sigma = 0$ at the surface and $\sigma = -1$, $z = -H$ at the bottom. The horizontal pressure gradient can be computed by

$$\frac{\partial p}{\partial x} = \frac{\partial p^*}{\partial x^*} - \frac{\sigma}{H} \frac{\partial H}{\partial x^*} \frac{\partial p^*}{\partial \sigma}. \quad (2)$$

The horizontal pressure gradient becomes difference between two large terms, which may cause two problems: (1) truncation error at steep topography [e.g., *Gary*, 1973; *Haney*, 1991; *Mellor et al.*, 1994, 1998; *McCalpin*, 1994; *Chu and Fan*, 1997, 1998; *Song*, 1998], and (2) hydrostatic inconsistency [e.g., *Mesinger*, 1984; *Haney*, 1991].

A consensus is reached in the ocean modeling community that the first problem does exist and several methods have been suggested to reduce the truncation errors to acceptable levels: (1) smoothing topography [e.g., *Chu and Fan*, 2001], (2) subtracting a mean vertical density profile before calculating the gradient [*Gary*, 1973], (3) bringing certain symmetries of the continuous forms into the discrete level to ensure cancellations of these terms such as the density Jacobian scheme [e.g., *Mellor et al.* 1998; *Song*, 1998;

Song and Wright, 1998], (4) increasing numerical accuracy [e.g., *McCalpin*, 1994; *Chu and Fan*, 1997, 1998, 1999, 2000, 2001], (5) changing the grid from a sigma grid to a z-level grid before calculating the horizontal pressure gradient [e.g., *Stelling and van Kester*, 1994]. *Kliem and Pietrzak* [1999] claimed that the z-level based pressure gradient calculation is the most simple and effective means to reduce the pressure gradient errors. However, *Ezer et al.* [2002] found that the density Jacobian scheme is more preferable.

No consensus is reached on whether the second problem exists. Based on the earlier work for atmospheric models [e.g., *Messiger*, 1982], *Haney* [1991] pointed out that the vertical discretization in sigma coordinate ocean models ($\delta\sigma$) should satisfy the hydrostatic consistency condition,

$$r \equiv \left| \frac{\sigma}{H} \frac{\delta_x H}{\delta\sigma} \right| < 1 \quad (3)$$

to keep the computational stability. Here r is the hydrostatic consistency parameter; $\delta_x H$ is the horizontal change in depth of adjacent grid cells; and $\delta\sigma$ is the vertical cell size associated with a sigma grid, $\delta x \delta\sigma$. However, *Mellor et al.* [1994] thought that r is just another measure of the numerical accuracy after conducting a numerical simulation for the North Atlantic Ocean using the Princeton Ocean Model with $r = 3$. More numerical experiments with various schemes for the seamount test case [e.g., *Ezer et al.*, 2002] were conducted to show convergent solutions with $r = 14.2$. These experiments show that the condition (3) is not the ultimate condition for numerical calculation, but the indication of the first (second) term in the righthand-side of (2) is larger if $r < 1$ ($r > 1$).

Does the hydrostatic inconsistency regarding to the computational instability really exist? We use the finite volume integration approach [*Lin*, 1997] to reexamine the concept of hydrostatic consistency (regarding the stability) in this paper. A fully,

hydrostatically consistent (i.e., hydrostatically stable) grid scheme is developed for sigma coordinate ocean models. This scheme provides a criterion for the identification of hydrostatic consistency for various finite difference schemes. The outline of this part is as follows: Description of the hydrostatic consistency is given in section 2. A hydrostatically consistent staggered scheme for horizontal pressure gradient is given in Section 3. Evidence of second-order staggered sigma ocean model is always hydrostatically consistent is given in Sections 4 and 5. In section 6, the conclusions are presented.

2. Hydrostatic Consistency

Let the flow field change in $x-z$ plane only (Fig. 1). A finite volume (trapezoidal cylinder) is considered with the length of L_y (in the y -direction) and the cross-section represented by the shaded region (trapezoid) in Figure 1. The resultant pressure force (\mathbf{F}) acting on the finite volume is computed as follows:

$$\mathbf{F} = L_y \oint_C p \mathbf{n} ds \quad (4)$$

where p is the pressure, C represents the four boundaries, \mathbf{n} denotes the normal unit vector pointing inward, and ds is an element of the boundary. The contour integral is taken counter-clockwise along the peripheral of the volume element. The pressure force exerts on boundaries of the finite-volume with p_w , p_e , p_u , and p_l on the west, east, upper, and lower sides. The horizontal (F_x) and vertical (F_z) components of the resultant pressure force are computed by

$$F_x = -L_y \left(\int_1^2 p_l dz + \int_2^3 p_e dz + \int_3^4 p_u dz + \int_4^1 p_w dz \right), \quad (5)$$

$$F_z = L_y \left(\int_1^2 p_l dx + \int_3^4 p_u dx \right), \quad (6)$$

where points 1, 2, 3, and 4 are the four vertices of the finite volume. For hydrostatic balanced models, the following condition must hold

$$F_z = g\Delta m, \quad (7)$$

where g is the gravitational acceleration, Δm is the mass of the finite volume. Equation (7) states that the vertical component of the resultant pressure force acting on the finite volume exactly balances the total weight of the finite volume.

For a Boussinesq, hydrostatic ocean model, the pressure field is given by

$$p = p_{atm} + \rho_0 g \eta + g \int_z^0 \rho(x, z', t) dz', \quad (8)$$

where p_{atm} is the atmospheric pressure at the ocean surface, ρ_0 is the characteristic density, and η is the surface elevation. Substitution of (8) into (6) leads to

$$\begin{aligned} F_z &= gL_y \left(\int_1^2 \int_z^0 \rho(x, z', t) dz' dx + \int_3^4 \int_z^0 \rho(x, z', t) dz' dx \right) \\ &= gL_y \iint_{\Delta S} \rho(x, z', t) dz' dx = g\Delta m, \end{aligned} \quad (9)$$

where ΔS is the area of the trapezoid (Fig. 1) computed by

$$\Delta S = (x_{i+1} - x_i) \cdot (z_{i,k} + z_{i+1,k} - z_{i,k+1} - z_{i+1,k+1}), \quad z_{i,k} = H_i \cdot \sigma_k. \quad (10)$$

Eq.(9) indicates that the finite-volume discretization guarantees the hydrostatic balance in Boussinesq, hydrostatic ocean models. Using (5) the horizontal pressure gradient is computed by

$$\frac{\partial p}{\partial x} \equiv \frac{F_x}{L_y \Delta S} = -\frac{1}{\Delta S} \left(\int_1^2 p_l dz + \int_2^3 p_e dz + \int_3^4 p_u dz + \int_4^1 p_w dz \right). \quad (11)$$

If the horizontal pressure gradient is represented by (11), the model is conserved and hydrostatic inconsistency does not exist. Thus, deviation from the hydrostatic consistency becomes deviation of the horizontal pressure gradient computation from (11).

3. Staggered Grid

The staggered grid is represented in Figure 1 with the velocity at the center of the volume and pressure at the four vertices. Discretization of the horizontal pressure gradient with the finite-volume consideration (11) is given by

$$\frac{\Delta p}{\Delta x} = \frac{1}{\Delta S} \left[\bar{p}_l (z_{i+1,k+1} - z_{i,k+1}) + \bar{p}_e (z_{i+1,k} - z_{i+1,k+1}) + \bar{p}_u (z_{i,k} - z_{i+1,k}) + \bar{p}_w (z_{i,k+1} - z_{i,k}) \right], \quad (12)$$

where $\bar{p}_l, \bar{p}_e, \bar{p}_u, \bar{p}_w$ are the mean values of pressure at the four sides of the trapezoid. Equation (12) is the criterion for justifying the hydrostatic consistency for ocean model with staggered grid. If the horizontal pressure gradient in sigma coordinates (2) can be represented by (12), the model is hydrostatically consistent. Otherwise the model may be hydrostatically inconsistent. For ocean models with C-grid, the two consecutive finite-volumes are considered as one volume (Fig. 2). The hydrostatic consistency can be easily evaluated on these finite-volumes.

4. Second-Order Accuracy

For the second-order staggered grid, $\bar{p}_l, \bar{p}_e, \bar{p}_u, \bar{p}_w$, are taken as the arithmetic means of pressure at the two vertices,

$$\bar{p}_w = \frac{p_{i,k} + p_{i,k+1}}{2}, \quad \bar{p}_e = \frac{p_{i+1,k} + p_{i+1,k+1}}{2},$$

$$\bar{p}_l = \frac{p_{i,k+1} + p_{i+1,k+1}}{2} \quad \bar{p}_u = \frac{p_{i,k} + p_{i+1,k}}{2}. \quad (13)$$

Substitution of (13) into (12) leads to

$$\left(\frac{\Delta p}{\Delta x} \right)_{i,k} = \frac{(p_{i+1,k+1} - p_{i,k}) \cdot (H_{i+1} \sigma_k - H_i \sigma_{k+1}) + (p_{i+1,k} - p_{i,k+1}) \cdot (H_i \sigma_k - H_{i+1} \sigma_{k+1})}{\delta x_i \cdot \delta \sigma_k \cdot (H_i + H_{i+1})}, \quad (14)$$

where $\delta x_i = x_{i+1} - x_i$ and $\delta \sigma_k = \sigma_k - \sigma_{k+1}$. Equation (14) is the discretization of the horizontal pressure gradient with the finite-volume consideration.

5. Finite Difference Scheme

Finite difference schemes are commonly used in sigma coordinate ocean models.

Using the central difference scheme, the horizontal pressure gradient (2) is discretized by

$$\begin{aligned} \left(\frac{\delta p}{\delta x} \right)_{i,k} &= \frac{p_{i+1,k} + p_{i+1,k+1} - p_{i,k} - p_{i,k+1}}{2 \cdot \delta x_i} - \frac{\sigma_k + \sigma_{k+1}}{H_i + H_{i+1}} \cdot \frac{H_{i+1} - H_i}{\delta x_i} \cdot \frac{p_{i,k} + p_{i+1,k} - p_{i,k+1} - p_{i+1,k+1}}{2 \cdot \delta \sigma_k} \\ &= \frac{(p_{i+1,k+1} - p_{i,k}) \cdot (H_{i+1} \sigma_k - H_i \sigma_{k+1}) + (p_{i+1,k} - p_{i,k+1}) \cdot (H_i \sigma_k - H_{i+1} \sigma_{k+1})}{\delta x_i \cdot \delta \sigma_k \cdot (H_i + H_{i+1})}, \end{aligned} \quad (15)$$

which is exactly the same as (14). This means that the sigma coordinate ocean models with second-order staggered grid is always hydrostatically consistent. This confirms Mellor et al.'s [1994] claim that the hydrostatic consistency is irrelevant any way in the sigma coordinate ocean models and that the hydrostatic consistency parameter r is just another measure of the numerical errors.

6. Conclusions

(1) Using the finite-volume integration approach, a hydrostatically consistent, discrete scheme [equation (12)] is obtained to compute horizontal pressure gradient. For the second-order accuracy, this scheme is exactly the same as the commonly used sigma coordinate ocean models (staggered grids) with the second-order central difference scheme. This indicates that the current sigma coordinate ocean models with second order staggered scheme are always hydrostatically consistent.

(2) Deviation of discretization schemes for computing the horizontal pressure gradient from equation (12) can be taken as a measure for hydrostatic inconsistency. The larger the deviation, the larger the hydrostatic inconsistency is.

(3) Equation (12) provides the guidance for establishing hydrostatically consistent schemes for horizontal pressure gradient. More accurate schemes should be developed on the base of accurate estimate of mean pressure at four sides of the finite-volume (i.e., $\bar{p}_l, \bar{p}_e, \bar{p}_u, \bar{p}_w$).

Acknowledgements

This study was supported by the Office of Naval Research, the Naval Oceanographic Office, and the Naval Postgraduate School.

References

Beckmann, A., and D. B. Haidvogel, Numerical simulation of flow around a tall isolated seamount. Part 1: Problem formulation and model accuracy. *J. Phys. Oceanogr.*, **23**, 1736-1753, 1993.

Chu, P.C., and C.W. Fan, Sixth-order difference scheme for sigma coordinate ocean models. *J. Phys. Oceanogr.*, **27**, 2064-2071, 1997.

Chu, P.C., and C.W. Fan, A three-point combined compact difference scheme. *J. Comput. Phys.* 140, 370-399, 1998.

Chu, P.C., and C. Fan, A three-point sixth-order nonuniform combined compact difference scheme. *J. Comput. Phys.*, 148, 663-674, 1999.

Chu, P.C., and C.W. Fan, A staggered three-point combined compact difference scheme. *Math. Comput. Modeling*, **32**, 323-340, 2000.

Chu, P.C., and C.W. Fan, An accuracy progressive sixth-order finite- difference scheme. *J. Atmos. Oceanic Technol.*, 18, 1245-1257, 2001.

Ezer, T., H. Arango, A.F. Shchepetkin, Developments in terrain-following ocean models: intercomparisons of numerical aspects. *Ocean Modelling*, 4, 249-267, 2002.

Gary, J.M., Estimate of truncation error in transformed coordinate primitive equation atmospheric models. *J. Atmos. Sci.*, **30**, 223-233, 1973.

Haney, R.L., On the pressure gradient force over steep topography in sigma coordinate ocean models. *J. Phys. Oceanogr.*, **21**, 610-619, 1991.

Kliem, N., and J.D. Pietrzak, On the pressure gradient error in sigma coordinate ocean models: A comparison with a laboratory experiment. *J. Geophys. Res.*, **104**, 29781-29799, 1999.

Lin, S.-J., A finite volume integration method for computing pressure gradient force in general vertical coordinates. *Q. J. R. Meteorol. Soc.*, **123**, 1749-1762, 1997.

McCalpin, J.D., A comparison of second-order and fourth-order pressure gradient algorithms in a sigma-coordinate ocean model. *Inter. J. Num. Methods in Fluids*, **18**, 361-383, 1994.

Mellor, G.L., T. Ezer, and L.-Y. Oey, The pressure gradient conundrum of sigma coordinate ocean models. *J. Atmos. Oceanic Technol.*, **11**, 1126-1134, 1994.

Mellor, G.L., L.-Y. Oey and T. Ezer, Sigma coordinate pressure gradient errors and the seamount problem. *J. Atmos. Oceanic Technol.*, **15**, 1122-1131, 1998.

Song, Y.T., A general pressure gradient formulation for ocean models. Part 1: Scheme design and diagnostic analysis. *Mon. Wea. Rev.*, **126**, 3213-3230, 1998.

Song, Y.T., and D.G. Wright, A general pressure gradient formulation for the ocean models. Part 2: Momentum and bottom torque consistency. *Mon. Wea. Rev.*, **126**, 3213-3230, 1998.

Stelling, G.S., and J.A.T.M. van Kester, On the approximation of horizontal gradients in sigma coordinates for bathymetry with steep bottom slope. *Int. J. Numer. Methods Fluids*, **18**, 915-935, 1994.

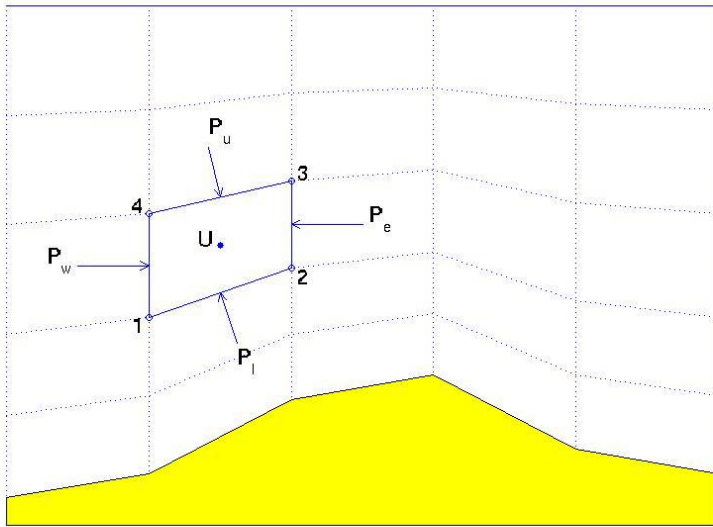


Figure 1. Finite-volume discretization and staggered grid in terrain-following coordinates with two cells representing $r > 1$ and $r < 1$.

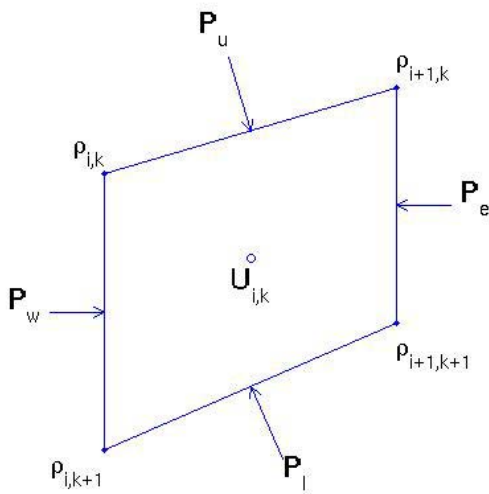


Figure 2. Double finite-volumes for C-grid.